Valence fluctuations and correlated metallic states in *A*-site ordered perovskite oxides $ACu_3V_4O_{12}$ (A=Na, Ca, and Y)

Yosuke Morita,[1] Takaaki Sudayama,[1] Kou Takubo,[1] Hiroshi Shiraki,[2] Takashi Saito,[2] Yuichi Shimakawa,[2] and Takashi Mizokawa[1]

[1]*Department of Physics and Department of Complexity Science and Engineering, University of Tokyo, Kashiwa, Chiba 277-8561, Japan*

[2]*Institute for Chemical Research, Kyoto University, Uji, Kyoto 611-0011, Japan*

(Received 20 August 2009; revised manuscript received 22 March 2010; published 20 April 2010)

We have studied the electronic structure of *A*-site ordered perovskite oxides $ACu_3V_4O_{12}$ (A=Na, Ca, and Y) using photoemission spectroscopy. V and Cu valence fluctuations are clearly observed in the V $2p$ and the Cu $2p$ core-level spectra. In going from A=Na to Ca to Y, electrons doped by the *A*-site substitution are mainly captured by the Cu site which has a mixture of $+2(d^9)$ and $+3$ (d^9L, L is an O $2p$ hole) and are partly distributed into the V site. The photoemission spectra near the Fermi level show a systematic change induced by the *A*-site substitution. The electronic structure of $ACu_3V_4O_{12}$ is very different from that in $Ca_{1-x}Sr_xVO_3$ due to the existence of the Cu $3d$ electrons, and the unusual correlation effect in $ACu_3V_4O_{12}$ can be related to the valence fluctuations observed in the core-level spectra.

DOI: 10.1103/PhysRevB.81.165111 PACS number(s): 71.30.+h, 79.60.−i, 71.28.+d

I. INTRODUCTION

In the last two decades, physical properties of transition-metal oxides with perovskite structure ABO_3 have been studied intensively and extensively.[1] The interesting physical properties including superconductivity, colossal magnetoresistance, metal-insulator transitions, and multiferroic behaviors are partly derived from the flexibility of the BO_6 octahedron which allows various distortions such as the tilting, elongation, and compression.[2] Among the ABO_3 compounds, $Ca_{1-x}Sr_xVO_3$ has been attracting much interest because of the proximity to the Mott transition and the bandwidth control due to the tilting of VO_6 octahedron, and the correlation effect in the V $3d$ band has been revealed by means of photoemission spectroscopy.[3–8]

Recently, a variety of *A*-site ordered perovskite-type oxides $ACu_3B_4O_{12}$ have been found to show interesting physical properties which are not obtained in ABO_3.[9] For example, $CaCu_3Ti_4O_{12}$ exhibits an enhanced dielectric property and an interesting magnetic state.[10–12] $ACu_3Ru_4O_{12}$ (A=Na, Ca, and La) shows a *d*-electron heavy-fermion behavior with enhanced electronic specific coefficients.[13–15] $CaCu_3Fe_4O_{12}$ and $LaCu_3Fe_4O_{12}$ show novel charge-ordering and/or charge-transfer transitions.[16,17] In $ACu_3B_4O_{12}$, three quarters of *A* sites are occupied by Cu ions and the BO_6 octahedra are tilted to stabilize the Cu^{2+} ions with the pseudosquare planar coordination. However, the valence or the electronic configuration of the Cu ions in $ACu_3B_4O_{12}$ has not been studied systematically using spectroscopic methods except $CaCu_3Ru_4O_{12}$ and $CaCu_3Ti_4O_{12}$, which are reported to have Cu^{2+} (d^9),[18–20] and $ACu_3Co_4O_{12}$ (A=Ca and Y), which are reported to have Cu^{3+} (d^9L).[21] In the present work, we report on a photoemission study of $ACu_3V_4O_{12}$ (A=Na, Ca, and Y) which show metallic resistivities with Pauli paramagnetic behaviors. The electronic specific-heat coefficient γ of $ACu_3V_4O_{12}$ are moderately enhanced to 30–50 $mJ/mol/K^2$, and the Wilson ratio is around 2 which is the typical value for heavy-fermion systems, indicating that electron-electron interactions play important roles to realize the correlated metallic states in *A*-site ordered perovskite oxides $ACu_3V_4O_{12}$.[22] Since the V-O-V bond angle is 142.11°, 142.22°, and 142.31° for A=Na, Ca, and Y,[22] the variation in the V-O-V bond angle induced by *A*-site substitution is much smaller in $ACu_3V_4O_{12}$ than that in $Ca_{1-x}Sr_xVO_3$. The present photoemission study reveals that the Cu valence is a mixture of +2 (d^9 configuration) and +3 (d^9L configuration, L represents an O $2p$ hole) and that the V valence is a mixture of $+3(d^2)$ and $+4(d^1)$. On the basis of the photoemission results, we argue that the electronic structure of $ACu_3V_4O_{12}$ is very different from that of $Ca_{1-x}Sr_xVO_3$ and that the correlated metallic state is characterized by the valence fluctuations.

II. EXPERIMENTS

The polycrystalline samples of $NaCu_3V_4O_{12}$, $CaCu_3V_4O_{12}$, and $YCu_3V_4O_{12}$ were prepared by a solid-state reaction as described in the literature.[22] The polycrystalline samples were fractured *in situ* to obtain clean surfaces. X-ray photoemission spectroscopy (XPS) measurements were performed at room temperature using the JPS9200 electron analyzer. Monochromatic Al $K\alpha$ (1486.6 eV) was used as an x-ray source. The pass energy of the electron analyzer was set to 10 eV. The total-energy resolution including the x-ray source and the electron analyzer was ~0.6 eV. The binding energy was calibrated using the Fermi edge and the Au $4f$ core level of gold reference samples. The base pressure of the XPS chamber was 1×10^{-7} Pa. The ultraviolet photoemission spectroscopy (UPS) measurements were carried out at room temperature using SES-100 electron analyzer. He I (21.2 eV) was used as a light source. The energy resolution was set to 30 meV. The binding energy was calibrated using the Fermi edge of gold reference samples. The base pressure of the UPS chamber was 1×10^{-7} Pa.

III. RESULTS AND DISCUSSION

Figure 1 shows the XPS results for V $2p$ and O $1s$ core levels of $ACu_3V_4O_{12}$ (A=Na, Ca, and Y). The O $1s$ core-

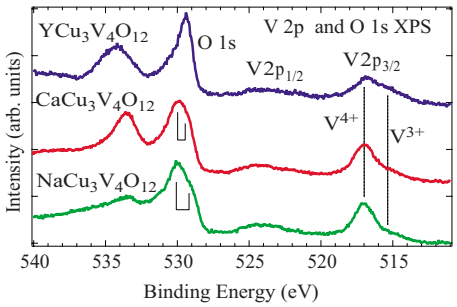

FIG. 1. (Color online) O 1*s* and V 2*p* core-level XPS spectra of $ACu_3V_4O_{12}$ (A=Na, Ca, and Y) taken at room temperature. The broad peak at ~533–534 eV is derived from grain boundaries at the surface region. The O 1*s* main peak at ~529–530 eV is split into two components for A=Ca and Na. V 2*p* peaks are split into two components representing the V valence fluctuations.

level peaks are located at ~529–530 and ~533–534 eV. The broad peak at ~533–534 eV is mainly derived from grain boundaries at the surface region. The thickness of the grain-boundary region at the surface probably increases in going from Na to Ca to Y. The O 1*s* main peak at ~529–530 eV becomes broader in going from A=Y to Ca to Na. The energy splitting of the O 1*s* main peak is caused by the screening effect on the O 1*s* core hole due to the O 2*p* electrons involved in the electronic states near the Fermi level (E_F). Namely, the O 2*p* component in the near-E_F electronic states becomes larger in going from A=Y to Ca to Na. This interpretation is consistent with the result of the Cu 2*p* XPS which shows the d^9L state increases in going from A=Y to Ca to Na. The V $2p_{3/2}$ and $2p_{1/2}$ peaks are accompanied by shoulders on the lower binding-energy side. It is possible to assign the shoulder structure to the V^{3+} component and the main peak to the V^{4+} component. Such core-level splitting is widely observed in various metallic V oxides such as $Li_{1-x}Zn_xV_2O_4$.[23]

Figure 2 shows the Cu 2*p* core-level XPS spectra of $ACu_3V_4O_{12}$ (A=Na, Ca, and Y). The Cu $2p_{3/2}$ and $2p_{1/2}$ peaks are split into the main and satellite structures which are

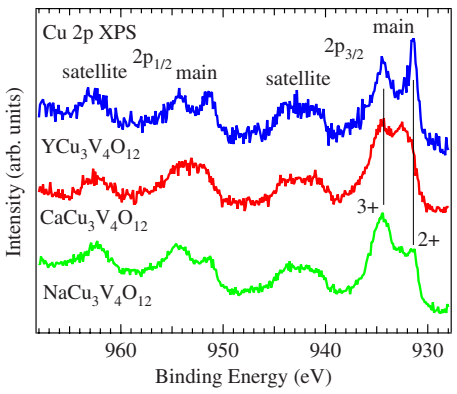

FIG. 2. (Color online) Cu 2*p* core-level XPS spectra of $ACu_3V_4O_{12}$ (A=Na, Ca, and Y) taken at room temperature. The splitting between the main and satellite structures is derived from the charge-transfer screening process of the Cu 2*p* core hole. The Cu 2*p* main peaks are further split into two components representing the Cu valence fluctuations.

derived from the charge-transfer screening process of the Cu 2*p* core hole. The Cu 2*p* main structures are made up from two components which can be attributed to Cu^{2+} and Cu^{3+} components. The lower binding-energy component is located at ~932 eV and can be attributed to the Cu^{2+} site with d^9 configuration. The higher binding-energy component at ~934 eV is similar to the Cu 2*p* peak position of $NaCuO_2$ (Refs. 24 and 25) and $LaCuO_3$,[26] where the Cu valence is formally +3 and the Cu ion takes the d^9L configuration that corresponds to the Zhang-Rice singlet state. The observation of Cu^{3+} is apparently inconsistent with the fact that, in these A-site ordered perovskite oxides, Cu^{2+} state with d^9 configuration is stable due to the square planar coordination. However, the Zhang-Rice singlet state with the $d^9L(^1A_{1g})$ configuration is well stabilized by the square planar coordination compared to the triplet state with the $d^8(^3B_{1g})$ configuration. Therefore, the contribution of the O 2*p* hole is essential to stabilize the formally Cu^{3+} state with the square planar coordination.[27] The final states of the main and satellite structures for the Cu^{2+} (d^9) ground state correspond to $d^{10}L$ and d^9 configurations, respectively, and the final states of the main and satellite structures for the Cu^{3+} (d^9L) ground state roughly corresponds to $d^{10}L^2$ and d^9L configurations, respectively.

In the Cu 2*p* XPS spectra, the Cu 2*p* core hole is screened by the charge transfer from O 2*p* to Cu 3*d* orbitals. Namely, the number of the Cu 3*d* electrons in the final state for the Cu 2*p* XPS main peak is very different from that of the ground state. Since the Cu^{2+} and the Cu^{3+} ground states take d^9 and d^9L configurations, respectively, the charge-transfer effect on the Cu 2*p* core hole is different between Cu^{2+} and Cu^{3+}. In addition, the local and nonlocal charge-transfer effects give the well-screened and poorly screened features in the main peak even for the single valence Cu^{2+} ground state.[18,28] Therefore, the simple decomposition into the Cu^{2+} and Cu^{3+} peaks of the Cu 2*p* XPS spectra is not that reliable to estimate the Cu valence of the ground state. On the other hand, in the V 2*p* XPS spectra, the charge-transfer screening effect on the V 2*p* core hole is very small, and the estimated V valence from the decomposition into V^{3+} and V^{4+} peaks is relatively accurate. Here, it should be noted that metallic V oxides with edge-sharing VO_6 octahedra such as $V_{1-x}Cr_xO_2$ and LiV_2O_4 are known to show complicated V 2*p* line shapes mainly due to the screening process involving V 3*d* t_{2g} electrons of neighboring V sites.[29–31]

In Fig. 3, the V 2*p* XPS spectra of $ACu_3V_4O_{12}$ (A=Na, Ca, and Y) are decomposed into V^{3+} and V^{4+} components. The model spectral functions with two Gaussians for V^{3+} and V^{4+} components are fitted to the experimental results. Here, it should be noted that the spectral function of each V^{3+} and V^{4+} component is expected to deviate from the Gaussian form due to the multiplet structures of the V 2*p* core hole and V 3*d* electrons. Although the multiplet effect is neglected in the present analysis and obtained valence values are not that reliable, it is still useful to demonstrate the mixed-valence nature of the V site and the qualitative valence change by the A-site substitution. In the present analysis, the ratio between V^{3+} and V^{4+} components is about 1:4, 1:5, and 1:2 for A=Na, Ca, and Y, respectively. Therefore, the V valence is roughly estimated to be +3.8, +3.8, and +3.7

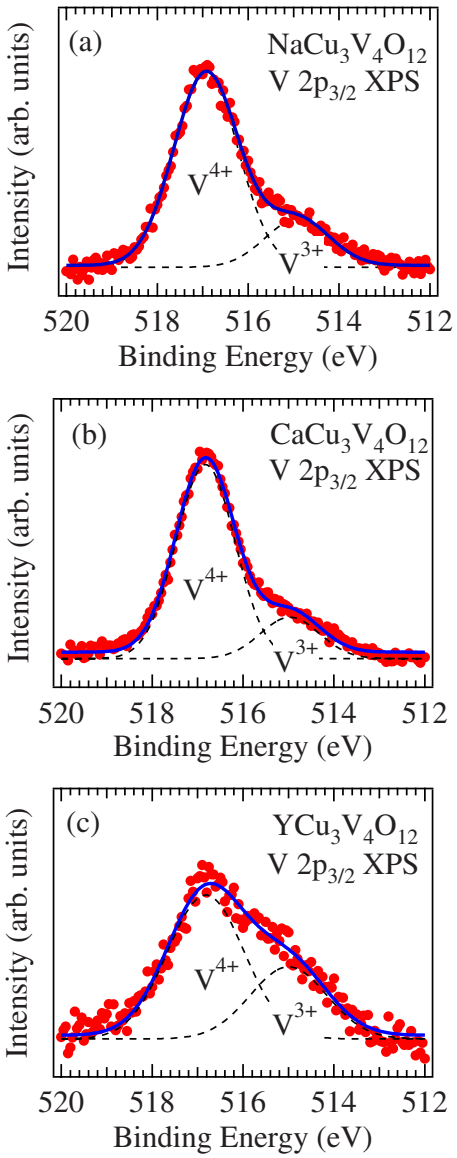

FIG. 3. (Color online) Fitted results (solid curves) for the V $2p$ spectra of (a) $NaCu_3V_4O_{12}$, (b) $CaCu_3V_4O_{12}$, and (c) $YCu_3V_4O_{12}$. The V $2p$ spectra are decomposed into V^{3+} and V^{4+} components as indicated by the dashed curves.

for A=Na, Ca, and Y. In the above valence estimation from the XPS spectra, the V valence does not change in going from A=Na to Ca. Therefore, it is expected that the Cu sites accommodate electrons doped by the substitution of Ca for Na. Actually, as shown in Fig. 2, the Cu^{3+} component is reduced in going from A=Na to Ca although quantitative analysis of the Cu $2p$ spectra is difficult as discussed in the previous paragraph. In going from A=Ca to Y, the V valence decreases from +3.8 to +3.7, indicating that electrons doped by the substitution of Y for Ca are accommodated by the V sites and the Cu sites. Figure 2 shows that the Cu^{3+} component is actually reduced in going from A=Ca to Y. The above estimation indicates that the filling of the V $3d$ band slightly increases from $d^{1.2}$ to $d^{1.2}$ to $d^{1.3}$ in going from A=Na to Ca to Y and that the doped electrons are mainly accommodated by the Cu site. The noninteger number of the V $3d$ electrons

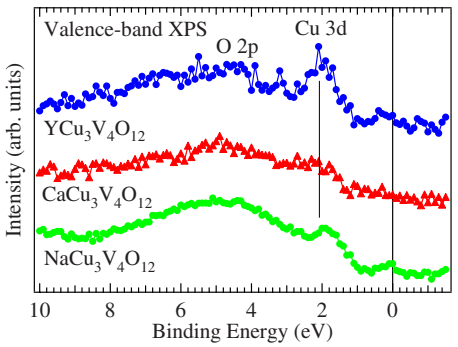

FIG. 4. (Color online) Valence-band XPS spectra of $ACu_3V_4O_{12}$ (A=Na, Ca, and Y) taken at room temperature.

per site indicates that the present systems are far from the Mott insulator of the V $3d$ electrons. Therefore, the correlation effect in the V $3d$ band could be very different from that in $Ca_{1-x}Sr_xVO_3$.[3–8]

Figure 4 shows the valence-band XPS spectra of $ACu_3V_4O_{12}$ (A=Na, Ca, and Y). As for the valence-band structure, the peaks at ~2 eV are derived from the Cu $3d$ band. The broad structure ranging from 3 to 8 eV can be attributed to the O $2p$ band hybridized with Cu $3d$ and V $3d$ orbitals. Considering the photoionization cross section of Cu $3d$ and O $2p$ subshells at the XPS measurements with Al $K\alpha$, the intensity of the O $2p$ band is mainly due to the Cu $3d$ component. The present result indicates that the hybridization strength between Cu $3d$ and O $2p$ orbitals gradually increases in going from A=Y to Ca to Na. Unfortunately, the photoionization cross section of the V $3d$ subshell is much smaller than that of the Cu $3d$ subshell, and, consequently, the V $3d$ band near E_F is not well detected in the XPS spectra. The Cu $3d$ peak is shifted to the higher binding-energy side in going from A=Na to Y, which is consistent with the electron doping by the A-site substitution. However, V $2p$ and O $1s$ core-level peaks tend to be shifted to the lower-energy side in going from A=Na to Y, which is not consistent with the rigid-band shift by the electron doping. It is difficult to explain the doping effect by the simple rigid-band picture. In the present system, the interplay between the V $3d$ bands and the Cu $3d$ (strongly hybridized with O $2p$) bands complicates the doping process.

The UPS spectra near E_F for A=Na, Ca, and Y are displayed in Fig. 5. The spectral feature ranging from 0 to 1.0 eV becomes narrower and the spectral weight at 0.2 eV becomes larger in going from Y to Ca to Na. For A=Na, the V $3d$ band has a peak at 0.2 eV well below E_F and the spectral weight at E_F seems to be suppressed compared to the peak height. Such spectral weight suppression at E_F is similar to the observation for $SrVO_3$ by Eguchi *et al.*[32] Consequently, although the peak height at 0.2 eV below E_F increases from Y to Ca to Na, the spectral weight at E_F does not increase that much from Y to Ca to Na. The origin of the peak at 0.2 eV would be related to the increase in the d^9L (Zhang-Rice singlet) state suggested by O $1s$ and Cu $2p$ XPS spectra. Namely, the increase in the d^9L state changes the hybridization between the V $3d$ band near E_F and the Cu $3d$ band at ~2 eV below E_F and, consequently, the shape of the V $3d$ band is changed. Theoretical studies on Cu $3d$ and

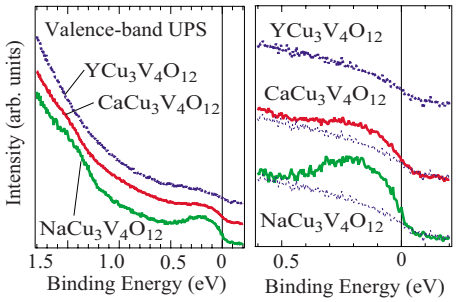

FIG. 5. (Color online) UPS spectra of $ACu_3V_4O_{12}$ (A=Na, Ca, and Y) taken at room temperature. In the right panel, the near-E_F spectra for A=Na and Ca are compared with that for A=Y shown by the dotted curves.

V 3d hybridization effect are required to further understand the origin of the spectral change by the A-site substitution.

In order to estimate the density of states at E_F from the experimental result, it is assumed that the spectral weight near E_F is derived from the V 3d band which has the band filling determined from the V 2p core-level spectra. We have extracted the V 3d band by subtracting the tail of the O 2p contribution from the experimental result. Here, the tail of the O 2p contribution is approximated by the power-law function. The V 2p XPS result shows that the V 3d band fillings are close to $d^{1.2}$ for A=Na and Ca, and $d^{1.3}$ for Y. Therefore, the numbers of V 3d electrons in the unit cell are $\sim 4 \times 1.2 = 4.8$ for A=Na and Ca, and 5.2 for A=Y. The integrated intensity of the obtained V 3d t_{2g} band divided by 4.8 or 5.2 corresponds to the spectral area per V 3d electron. The intensity at E_F can be estimated from the symmetrized spectrum where the effect of Fermi-Dirac distribution function is removed. The intensity at E_F divided by the spectral area per 3d electron and multiplied by Avogadro constant corresponds to the density of states $g(E_F)$ per formula unit. Assuming that the renormalization factor z is unity, the electronic specific-heat coefficient $\gamma = \frac{\pi^2}{3} k_B^2 g(E_F)$ per formula unit is estimated to be 10, 9.5, and 12 $\mathrm{mJ/eV/K^2}$ for A=Na, Ca, and Y, respectively. By comparing the estimated values with the experimental values of 50, 30 and 40 $\mathrm{mJ/mol/K^2}$ for A=Na, Ca, and Y, respectively,[22] the inverse of the renormalization factor $1/z$ is ~5, 3, and 3 for A=Na, Ca, and Y. These values are slightly larger than those for $Ca_{1-x}Sr_xVO_3$ with $1/z$ of 2–3.[33] Since the number of the V 3d electrons is 1.2–1.3 in $ACu_3V_4O_{12}$, the closeness to the Mott transition is not that important. The moderate mass renormalization is due to the electron-electron interactions in the V 3d band hybridized with Cu 3d and O 2p orbitals, and is related to the valence fluctuations observed in the core-level spectra. Since the present system includes the V 3d t_{2g} orbitals and the Cu 3d orbitals, one of the 3d band would be close to the orbital-selective Mott transition. The relationship between the valence fluctuation, orbital-selective Mott transition, and the mass renormalization is an interesting issue and the present system provides a unique playground for it.

IV. CONCLUSION

In summary, we have studied the electronic structure of A-site ordered perovskite oxides $ACu_3V_4O_{12}$ (A=Na, Ca, and Y) using photoemission spectroscopy. The V 2p and the Cu 2p core-level photoemission results show that the V and Cu valences are fluctuating. The carriers introduced by the substitution of A-site cation are mainly captured by the Cu site with a mixture of +2 (d^9) and +3 ($d^9\underline{L}$, $\underline{L}$ is an O 2p hole). The number of the V 3d electrons per V site is about 1.2–1.3 which is different from the integer number of the V 3d electrons in $Ca_{1-x}Sr_xVO_3$. The electronic structure of $ACu_3V_4O_{12}$ is different from that in $Ca_{1-x}Sr_xVO_3$ due to the existence of the Cu 3d electrons, and the correlated metallic state is characterized by the valence fluctuations of Cu and V sites.

ACKNOWLEDGMENTS

The authors would like to thank the valuable discussions with A. Fujimori, H. Wadati, M. Azuma, M. Mizumaki, and D. I. Khomskii. This work was supported by the Global COE program "the Physical Sciences Frontier" and the 21COE on the Kyoto Alliance for Chemistry from the Ministry of Education, Culture, Sports, Science, and Technology of Japan. It was also supported by Grants-in-Aid for Scientific Research from MEXT and from the Japan Society for the Promotion of Science (Grants No. 19GS0207 and No. 17105002).

[1] M. Imada, A. Fujimori, and Y. Tokura, Rev. Mod. Phys. **70**, 1039 (1998).
[2] P. M. Woodward, Acta Crystallogr., Sect. B: Struct. Sci. **53**, 32 (1997).
[3] A. Fujimori, I. Hase, H. Namatame, Y. Fujishima, Y. Tokura, H. Eisaki, S. Uchida, K. Takegahara, and F. M. F. de Groot, Phys. Rev. Lett. **69**, 1796 (1992).
[4] Y. Aiura, F. Iga, Y. Nishihara, H. Ohnuki, and H. Kato, Phys. Rev. B **47**, 6732 (1993).
[5] I. H. Inoue, I. Hase, Y. Aiura, A. Fujimori, Y. Haruyama, T. Maruyama, and Y. Nishihara, Phys. Rev. Lett. **74**, 2539 (1995).
[6] K. Morikawa, T. Mizokawa, K. Kobayashi, A. Fujimori, H. Eisaki, S. Uchida, F. Iga, and Y. Nishihara, Phys. Rev. B **52**, 13711 (1995).
[7] K. Maiti, P. Mahadevan, and D. D. Sarma, Phys. Rev. Lett. **80**, 2885 (1998).
[8] A. Sekiyama, H. Fujiwara, S. Imada, S. Suga, H. Eisaki, S. I. Uchida, K. Takegahara, H. Harima, Y. Saitoh, I. A. Nekrasov, G. Keller, D. E. Kondakov, A. V. Kozhevnikov, Th. Pruschke, K. Held, D. Vollhardt, and V. I. Anisimov, Phys. Rev. Lett. **93**, 156402 (2004).
[9] Y. Shimakawa, Inorg. Chem. **47**, 8562 (2008).
[10] M. A. Subramanian, D. Li, N. Duan, B. A. Reisner, and A. W. Sleight, J. Solid State Chem. **151**, 323 (2000).
[11] A. P. Ramirez, M. A. Subramanian, M. Gardel, G. Blumberg, D. Li, T. Vogt, and S. M. Shapiro, Solid State Commun. **115**, 217

(2000).
[12] C. C. Homes, T. Vogt, S. M. Shapiro, S. Wakimoto, and A. P. Ramirez, Science **293**, 673 (2001).
[13] W. Kobayashi, I. Terasaki, J. Takeya, I. Tsukada, and Y. Ando, J. Phys. Soc. Jpn. **73**, 2373 (2004).
[14] A. P. Ramirez, G. Lawes, D. Li, and M. A. Subramanian, Solid State Commun. **131**, 251 (2004).
[15] S. Tanaka, N. Shimazui, H. Takatsu, S. Yonezawa, and Y. Maeno, J. Phys. Soc. Jpn. **78**, 024706 (2009).
[16] I. Yamada, K. Takata, N. Hayashi, S. Shinohara, M. Azuma, S. Mori, S. Muranaka, Y. Shimakawa, and M. Takano, Angew. Chem., Int. Ed. **47**, 7032 (2008).
[17] Y. W. Long, N. Hayashi, T. Saito, M. Azuma, S. Muranaka, and Y. Shimakawa, Nature (London) **458**, 60 (2009).
[18] T. T. Tran, K. Takubo, T. Mizokawa, W. Kobayashi, and I. Terasaki, Phys. Rev. B **73**, 193105 (2006).
[19] M. Mizumaki, T. Saito, H. Shiraki, and Y. Shimakawa, Inorg. Chem. **48**, 3499 (2009).
[20] T. Sudayama, Y. Wakisaka, K. Takubo, T. Mizokawa, W. Kobayashi, I. Terasaki, S. Tanaka, Y. Maeno, M. Arita, H. Namatame, and M. Taniguchi, Phys. Rev. B **80**, 075113 (2009).
[21] T. Mizokawa, Y. Morita, T. Sudayama, K. Takubo, I. Yamada, M. Azuma, M. Takano, and Y. Shimakawa, Phys. Rev. B **80**, 125105 (2009).
[22] H. Shiraki, T. Saito, M. Azuma, and Y. Shimakawa, J. Phys. Soc. Jpn. **77**, 064705 (2008).
[23] A. Fujimori, K. Kawakami, and N. Tsuda, Phys. Rev. B **38**, 7889 (1988).
[24] T. Mizokawa, H. Namatame, A. Fujimori, K. Akeyama, H. Kondoh, H. Kuroda, and N. Kosugi, Phys. Rev. Lett. **67**, 1638 (1991).
[25] T. Mizokawa, A. Fujimori, H. Namatame, K. Akeyama, and N. Kosugi, Phys. Rev. B **49**, 7193 (1994).
[26] T. Mizokawa, A. Fujimori, H. Namatame, Y. Takeda, and M. Takano, Phys. Rev. B **57**, 9550 (1998).
[27] H. Eskes, L. H. Tjeng, and G. A. Sawatzky, Phys. Rev. B **41**, 288 (1990).
[28] M. A. van Veenendaal and G. A. Sawatzky, Phys. Rev. Lett. **70**, 2459 (1993).
[29] K. E. Smith and V. E. Henrich, Phys. Rev. B **50**, 1382 (1994).
[30] M. Taguchi, A. Chainani, N. Kamakura, K. Horiba, Y. Takata, M. Yabashi, K. Tamasaku, Y. Nishino, D. Miwa, T. Ishikawa, S. Shin, E. Ikenaga, T. Yokoya, K. Kobayashi, T. Mochiku, K. Hirata, and K. Motoya, Phys. Rev. B **71**, 155102 (2005).
[31] K. Takubo, J.-Y. Son, T. Mizokawa, H. Ueda, M. Isobe, Y. Matsushita, and Y. Ueda, Phys. Rev. B **74**, 155103 (2006).
[32] R. Eguchi, T. Kiss, S. Tsuda, T. Shimojima, T. Mizokami, T. Yokoya, A. Chainani, S. Shin, I. H. Inoue, T. Togashi, S. Watanabe, C. Q. Zhang, C. T. Chen, M. Arita, K. Shimada, H. Namatame, and M. Taniguchi, Phys. Rev. Lett. **96**, 076402 (2006).
[33] I. H. Inoue, O. Goto, H. Makino, N. E. Hussey, and M. Ishikawa, Phys. Rev. B **58**, 4372 (1998).